Supramolecular Chemistry
Publication details, including instructions for authors and subscription information:
http://www.informaworld.com/smpp/title~content=t713649759

Inclusion complexes of β-cyclodextrin with pyrazinamide and piperazine: Crystallographic and theoretical studies

Thammarat Aree[a]; Narongsak Chaichit[b]
[a] Department of Chemistry, Faculty of Science, Chulalongkorn University, Bangkok, Thailand [b] Department of Physics, Faculty of Science and Technology, Thammasat University, Pathum Thani, Thailand

To cite this Article Aree, Thammarat and Chaichit, Narongsak(2009) 'Inclusion complexes of β-cyclodextrin with pyrazinamide and piperazine: Crystallographic and theoretical studies', Supramolecular Chemistry, 21: 5, 384 — 393
To link to this Article: DOI: 10.1080/10610270802061184
URL: http://dx.doi.org/10.1080/10610270802061184

Supramolecular Chemistry
Vol. 21, No. 5, July–August 2009, 384–393

Taylor & Francis
Taylor & Francis Group

Inclusion complexes of β-cyclodextrin with pyrazinamide and piperazine: Crystallographic and theoretical studies

Thammarat Aree[a]* and Narongsak Chaichit[b]

[a]*Department of Chemistry, Faculty of Science, Chulalongkorn University, Phyathai Road, Pathumwan, Bangkok, Thailand;*
[b]*Department of Physics, Faculty of Science and Technology, Thammasat University, Rangsit, Pathum Thani, Thailand*

(*Received 25 December 2007; final version received 7 March 2008*)

The inclusion complexes of β-cyclodextrin (β-CD) with pyrazinamide (PYA) and piperazine (PIZ) have been investigated both in the solid phase by single-crystal X-ray diffraction analysis and in the gas phase by semi-empirical PM3 calculation. In the crystalline phase, the disordered PYA and PIZ molecules are entirely embedded in the β-CD cavity. The PYA pyrazine-centre displaces upwards by 1.15(1) Å from the β-CD plane, whereas the PIZ centre shifts downwards by 0.76(1) Å from the β-CD plane. The inclusion scenario changed in the gas phase. Two inclusion geometries of the PYA molecule are comparatively stable with binding energies of -22.28 and $-25.29\,\mathrm{kJ\,mol^{-1}}$: the pyrazine centre shifts upwards by 0.5 Å and downwards by 2.0 Å from the β-CD plane. The PIZ molecule positioning at 2.0 Å below the β-CD plane gives a more stable inclusion complex than does the PYA molecule by $22–25\,\mathrm{kJ\,mol^{-1}}$.

Keywords: β-cyclodextrin; inclusion complex; pyrazinamide; piperazine; crystal structure; PM3

Introduction

Cyclic oligosaccharides comprising 6-, 7- and 8-D-glucose units linked by α-(1→4)-glycosidic bonds are generally known as α-, β- and γ-cyclodextrins (CDs) (*1*). They resemble truncated cones and are amphiphilic with the hydrophobic cavity coated with C—H groups and O4, O5 atoms and the hydrophilic rims coated with O6—H groups on the narrower side and O2—H, O3—H groups on the wider side (Scheme 1).

CDs can form inclusion complexes (*2*) with a variety of guest molecules that fit partially or completely into the host CD cavity as shown by many CD crystal structures (*3*). They have applications in various industries (*4*), particularly in pharmacy to enhance aqueous solubility, chemical stability and bioavailability of poorly water-soluble drugs (*5*).

The CD inclusion complexes with pyrazinamide (PYA) and piperazine (PIZ) are rare in the literature. PYA is an antimicrobial tuberculosis drug while PIZ is used in the treatment of worm infections. Recently, Vinay has patented the improvement of the bioavailability of PYA upon inclusion complexation with β-CD in the solid phase (*6*). For the past two decades, Frömming and co-workers have investigated the inclusion complexes of PIZ with α-, β- and γ-CDs in the aqueous solution by NMR spectroscopy and revealed that PIZ forms a stable 1:1 complex exclusively with β-CD because of its optimum ring size, and not with the smaller α-CD ring nor the larger γ-CD ring (*7*, *8*). However, the chemical stability of PIZ against nitrosation is not improved in the presence of the three CDs (*8*). Because the inclusion complexes of β-CD with PYA and PIZ are not well understood, they deserve a more detailed investigation.

In the present work, we reveal a tangible evidence of the β-CD inclusion complexes with PYA and PIZ in the solid phase by single-crystal X-ray diffraction analysis and describe the formation of inclusion complexes using potential energy surfaces derived in the gas phase by semi-empirical Parametric Model 3 (PM3) calculation. The structural distinction of the inclusion complexes in the solid and gas phases is a paradigm of the CD conformational flexibility, the induced-fit mechanism and the dynamics of the inclusion process.

Experimental

Materials

β-CD purchased from Cyclolab (Budapest, Hungary), PYA from Sigma and PIZ from Fluka were used as received.

Crystal preparation

Crystallisation was commenced with dissolving 57 mg (0.05 mmol) of β-CD and 12.4 mg (0.10 mmol) of PYA or 8.7 mg (0.10 mmol) of PIZ in 1 ml of Milli-Q water at

*Corresponding author. Email: thammarat.aree@gmail.com

ISSN 1061-0278 print/ISSN 1029-0478 online

DOI: 10.1080/10610270802061184
http://www.informaworld.com

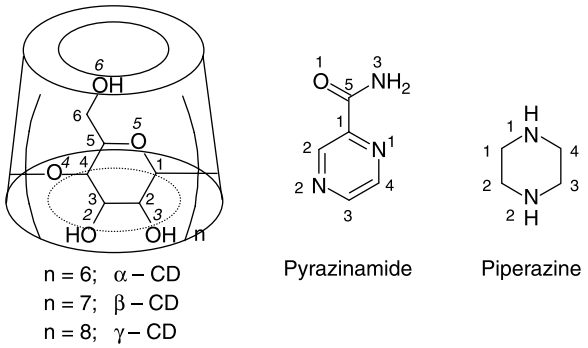

Scheme 1. Chemical structures and atomic numbering of CDs, PYA and PIZ.

60°C for 3 h. Then the saturated solution was allowed to cool down slowly to room temperature. Rod-like, colourless single crystals grew after a week of slow solvent evaporation.

X-ray diffraction analysis

A single crystal of each complex was mounted in a thin-walled glass capillary sealed at both ends by a trace of mother liquor. A total number of 17,885 reflections for the β-CD–PYA complex and 19,138 reflections for the β-CD–PIZ complex were collected to 0.75 Å resolution at 25°C using a SMART CCD (Bruker) with MoKα radiation (λ = 0.71073 Å) operating at a power of 50 kV and 30 mA. Data were reduced and empirical absorption corrections were applied with SHELXTL (*9*) and SADABS (*10*). Better crystal quality of the β-CD–PYA complex compared with that of the β-CD–PIZ complex gave rise to greater number of strong data with $F_o^2 > 2\sigma(F_o^2)$ and lower R_{int} (4890 vs. 2879 and 0.038 vs. 0.138; Table 1).

The crystal structures of both complexes were solved by molecular replacement with PATSEE (*11*) using the β-CD–acetic acid inclusion complex (*12*) as a phasing model. Only the atomic coordinates of β-CD skeleton,

Table 1. Summary of crystallographic data for the β-CD–PYA and β-CD–PIZ inclusion complexes.

	β-CD–PYA (**1**)	β-CD–PIZ (**2**)
Chemical formula	$(C_6H_{10}O_5)_7{\cdot}0.5C_5H_5N_3O{\cdot}5.5H_2O$	$(C_6H_{10}O_5)_7{\cdot}0.5C_4H_{10}N_2{\cdot}7.2H_2O$
Formula weight	1295.64	1307.78
Crystal habit, colour	Rod, colourless	Rod, colourless
Crystal size (mm^3)	0.2 × 0.2 × 0.5	0.2 × 0.3 × 0.5
Crystal system	Monoclinic	Monoclinic
Space group	$P2_1$	$P2_1$
Unit-cell dimensions		
a (Å)	20.831(1)	20.950(1)
b (Å)	10.294(1)	10.249(1)
c (Å)	15.216(5)	15.142(1)
β (°)	110.73(1)	108.76(1)
Volume ($Å^3$)	3051.4(1)	3078.7(1)
Z	2	2
D_x (g cm^{-3})	1.398	1.395
μ (mm^{-1})	0.13	0.13
F(000)	1356	1367
Diffractometer	SMART CCD (Bruker)	
Wavelength, MoKα (Å)	0.71073	
Temperature (°C)	25	
θ range for data collection (°)	8.20–28.28	
Resolution (Å)	0.75	
Measured reflections	17,885	19,138
Unique reflections	7372	7636
R_{int}	0.038	0.138
Index ranges	$0 \le h \le 27, -11 \le k \le 13, 0 \le l \le 20$	$0 \le h \le 27, -13 \le k \le 12, 0 \le l \le 20$
Unique reflections [$F^2 > 2\sigma(F^2)$]	4890	2879
Structure solution	Molecular replacement (PATSEE)	
Refinement method	Full-matrix least-squares on F^2	
Weighting scheme	$w = [S^2(F_o^2) + (0.1326P)^2 + 0.0261P]^{-1}$, where $P = (F_o^2 + 2F_c^2)/3$	$w = [S^2(F_o^2) + (0.0888P)^2 + 0.0049P]^{-1}$, where $P = (F_o^2 + 2F_c^2)/3$
Data/parameters	7372/858	7636/857
R [$F^2 > 2\sigma(F^2)$]	$R^a = 0.065$, $wR^b = 0.173$	$R^a = 0.093$, $wR^b = 0.167$
R (all data)	$R^a = 0.102$, $wR^b = 0.197$	$R^a = 0.229$, $wR^b = 0.249$
Goodness of fit	1.010	1.022
Highest peak/deepest hole (e $Å^{-3}$)	0.62/−0.34	0.30/−0.19

[a] $R = \sum||F_o| - |F_c||/\sum|F_o|$.

[b] $wR = \sum\{w(F_o^2 - F_c^2)^2/\sum w(F_o^2)^2\}^{1/2}$.

excluding O6 atoms, were used for the calculation. The β-CD O6 atoms, guests and water oxygen atoms were subsequently located by difference Fourier electron density maps assisted by the graphic programme XTALVIEW (*13*). All hydrogen atoms of β-CD, PYA and PIZ were placed at the theoretical positions according to the 'riding model' (*14*). The hydrogen atoms of freely rotated β-CD OH groups were included in the structure model solely for the correct estimates of the unit-cell content and crystal density. Hydrogen atoms of water molecules could not be determined. The structures were anisotropically refined by full-matrix least-squares on F^2 with SHELXL-97 (*14*) to converge at *R*-factors of 0.065 and 0.093 for the β-CD–PYA and the β-CD–PIZ inclusion complexes, respectively.

A summary of crystallographic data of both complexes is given in Table 1. The geometrical parameters including the glucose puckering parameters calculated with PARST (*15*) and PLATON (*16*) are listed in Tables 2–4. The final fractional atomic coordinates and equivalent isotropic thermal displacement factors are deposited at the Cambridge Crystallographic Data Centre (*17*).

Computational details

PM3 calculations

The starting structures of β-CD, PYA and PIZ, excluding H-atoms, were taken from the crystal structures obtained in the present X-ray diffraction analysis. Because the molecular structures of β-CD from both the complexes are nearly isomorphous (see below), we chose the β-CD atomic coordinates from the PYA complex with lower *R*-factor, i.e. more accurately determined. The atomic coordinates of β-CD, PYA and PIZ in the PDB format were completed with H-atoms, converted to GAUSSIAN Z-matrix using BABEL (*18*) and then fully optimised with PM3 calculation implemented in GAUSSIAN03 (*19*). The potential energy surface of the inclusion complex was computed by moving a guest molecule in a 1-Å step over (+*Z*) and beneath (−*Z*) the β-CD plane within a distance of 6 Å in each direction (Scheme 2). For the PYA molecule without a centre of symmetry, we considered two possible complexes with amide group pointing up and down: β-CD–PYA(u) and β-CD–PYA(d). For the PIZ molecule having a centre of symmetry, we considered one complex with the PIZ axis (N1–N2) perpendicular to the β-CD plane. At each 1-Å step, the complex was fully optimised with PM3 method. The binding energy of the complex was calculated from the differences between the PM3 energy of the complex and those of the free β-CD and drug. The potential energy surfaces of the β-CD–PYA(u), β-CD–PYA(d) and β-CD–PIZ complexes are given in Figure 3.

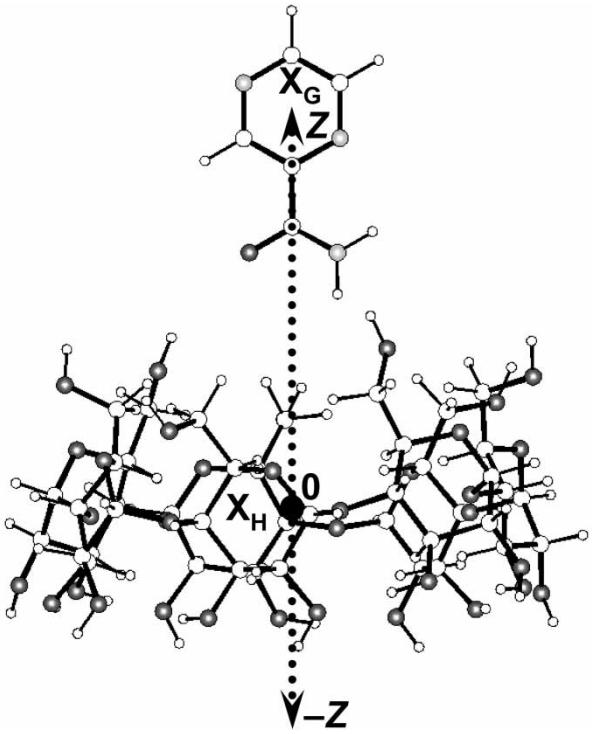

Scheme 2. Structure optimisation of the β-CD inclusion complexes with PM3 calculation. An example shown here is the β-CD–PYA complex with PYA amide group pointing down. Distance *Z* is measured from the centre of β-CD O4-plane (X_H, marked with solid circle) to the centre of pyrazine (X_G); 6 Å above and 6 Å below the O4-plane.

The overlays of PM3-optimised and crystal structures are depicted in Figure 4.

Results and discussion

Crystal structure description of inclusion complexes

General

β-CD co-crystallises with PYA and PIZ as β-CD·0.5PYA·5.5H_2O and β-CD·0.5PIZ·7.2H_2O, respectively, in the monoclinic space group $P2_1$ with comparable unit-cell dimensions. In the asymmetric unit, each complex comprises one β-CD, 0.5 PYA (or PIZ) and 5.5 (or 7.2) water molecules that are distributed over seven (or 11) positions. Water sites W1–W3 located in the β-CD cavity hydrogen bond to the guest molecule, while the remaining water sites are in the interstices between β-CD macrocycles. The β-CD structures in both complexes exhibit normal thermal motion with equivalent isotropic temperature factors (U_{eq}) of 0.037(1)–0.148(7) $Å^2$ for the β-CD backbone and 0.061(1)–0.24(3) $Å^2$ for the β-CD O6 atoms, whereas the guest molecules and some water sites show higher thermal motion with U_{eq} two times more (see ORTEP plots in Figure 1).

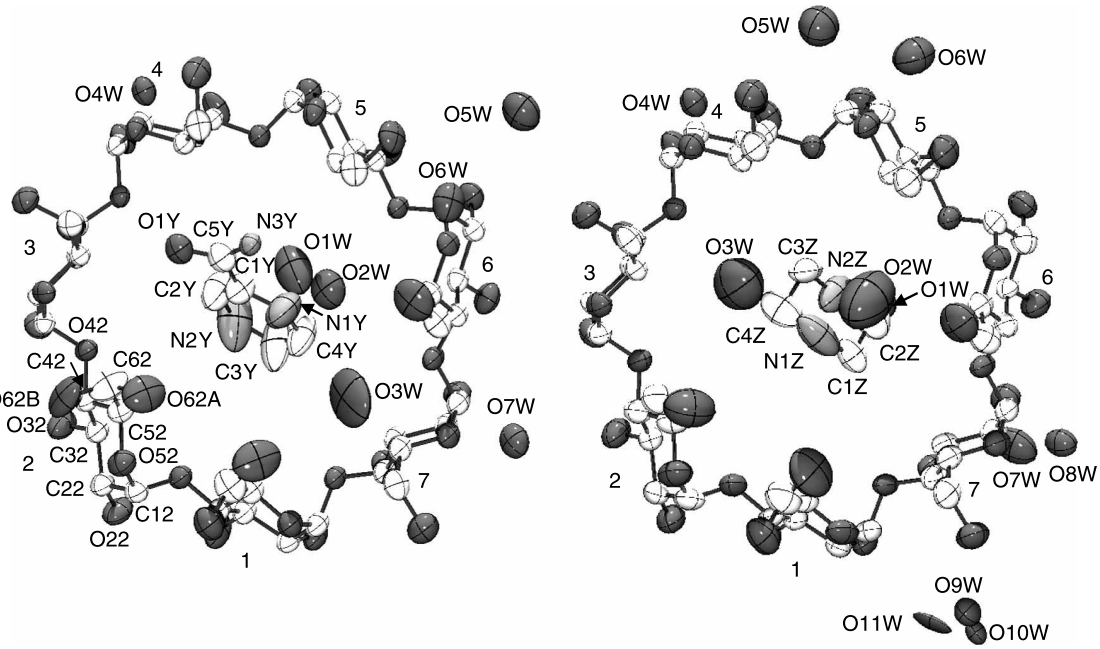

Figure 1. ORTEP plots (50% probability level) of (a) β-CD·0.5PYA·5.5H_2O (**1**) and (b) β-CD·0.5PIZ·7.2H_2O (**2**). C, white; O, dark grey; N, light grey; H, not shown. Atomic numbering is given for the glucose residue #2 of **1**. Drawn with GRETEP2 (*33*) and rendered with POV-RAY (*34*).

The atomic numbering scheme is that used conventionally for carbohydrates. The first number denotes the position in the glucose unit and the second number the glucose number in the CD macrocycle. Letters A and B indicate two-fold disorder. For example, O62A means the disordered O6 of glucose residue 2 (Scheme 1 and Figure 1). PYA is labelled with Y and PIZ with Z. The β-CD–PYA complex is denoted as **1** and the β-CD–PIZ as **2**.

The O···O and O···N distances of 3.5 Å are commonly used here and in our previous works (*12*) as a cut-off of 'possible' hydrogen bonding. This criterion covers the whole spectrum of strength levels from 'strong', 'moderate' to 'weak' hydrogen bonds with the corresponding separations of 2.2–2.5, 2.5–3.2 and ≥3.2 Å as categorised by Jeffrey (*20*).

β-CD macrocycles

The β-CD macrocycles of **1** and **2** are almost identical as indicated by very small rms deviation of superposition 0.083(1) Å (O6 atoms are excluded from the calculation). They adopt a 'round' conformation sustained by systematic intramolecular, interglucose O3(n)···O2(n + 1) hydrogen bonds with O···O distances (η) of 2.74(1)–3.01(1) Å for **1** and 2.79(1)–2.93(1) Å for **2** (Table 2, Figures 1 and 2). The circular conformation of β-CD is also evidenced by the short spans of torsion angles ϕ and ψ, angle ω at glycosidic O4, tilt angle τ and the small deviations of O4 from their common planes (distance δ; Table 2). The seven glucose units exhibit a regular $^4C_1$ chair conformation with Cremer–Pople puckering parameters Q and θ (*21*) of 0.54(1)–0.59(1) Å and 2.2(6)–5.5(6)° for **1** and 0.54(1)–0.57(1) Å and 2(1)–6(1)° for **2**, respectively. The β-CD O6—H groups are doubly disordered with occupancy factors for sites A and B: 0.59, 0.41 (O61—H of **1**); 0.76, 0.24 (O62—H of **1**); and 0.57, 0.43 (O61—H of **2**). The orientation of the C6—O6 groups is described by the torsion angle O5—C5—C6—O6 (γ) in Table 2. All C6—O6 groups direct 'away' from the β-CD cavity with the torsion angle γ ranging from −60.4(11) to −72.6(13)° (Table 2, Figures 1 and 2). Exceptions are the C61—O61B, C62—O62A and C66—O66 groups of **1** and the C61—O61B, C62—O62 and C66—O66 groups of **2** that point 'toward' the β-CD cavity with the torsion angle γ in the range of 57.1(7)–68.1(13)°. The β-CD O6—H groups in both the complexes are systematically hydrated with O···O separations of 2.69(2)–3.45(2) Å for **1** and 2.34(3)–3.21(2) Å for **2**. The water sites involved, listed sequentially from glucose #1–7, are: W2/W3, W1/W2, W4/W7, W5, W6, W3/W5/W6 and W6 for **1** and W1, W1, W4/W7/W8, W5, W6/W9/W10, W2/W5/W9/W11 and W9/W10 for **2** (Tables 3 and 4).

Table 2. Geometrical parameters of β-CD macrocycles in the PYA and PIZ inclusion complexes (distances in Å and angles in °).

Residue	1	2	3	4	5	6	7
Puckering							
Q[a]	0.54(1)	0.57(1)	0.54(1)	0.56(1)	0.59(1)	0.55(1)	0.56(1)
	0.54(1)	**0.57(1)**	**0.55(1)**	**0.55(1)**	**0.56(1)**	**0.54(1)**	**0.54(1)**
θ[b]	3.3(7)	3.6(6)	5.5(6)	2.5(5)	4.3(6)	4.7(6)	2.2(6)
	4(1)[c]	**2(1)**	**4(1)**	**2(1)**	**3(1)**	**6(1)**	**4(1)**
Angle							
ϕ[d]	115.8(5)	107.9(5)	102.9(5)	107.5(4)	113.2(4)	118.3(4)	104.2(5)
	113.5(9)	**108.6(10)**	**101.7(8)**	**107.9(7)**	**110.8(8)**	**119.5(7)**	**100.7(9)**
ψ[d]	139.8(5)	133.7(5)	116.9(5)	128.4(4)	127.4(4)	130.0(4)	113.3(5)
	140.5(9)	**132.0(9)**	**119.5(8)**	**129.9(7)**	**126.9(7)**	**129.8(7)**	**115.7(8)**
γ[e]	−70.4(8)[f]	60.4(8)[f]	−61.5(5)	−62.6(6)	−68.8(6)	57.1(7)	−64.0(5)
	64.6(12)[f]	−60.4(11)[f]					
	−72.6(13)[g]	**68.1(13)**	**−63.4(8)**	**−62.7(9)**	**−70.4(10)**	**59.5(13)**	**−65.7(9)**
	60.8(19)[g]						
τ[h]	15.9(4)	25.8(3)	10.2(3)	6.2(2)	11.3(3)	18.5(3)	4.3(3)
	17.1(7)	**25.4(6)**	**8.9(5)**	**8.3(4)**	**12.0(4)**	**21.1(5)**	**2.8(5)**
ω[i]	128.5(1)	128.7(1)	124.6(1)	132.2(1)	128.9(1)	125.1(1)	130.5(1)
	128.6(2)	**127.6(2)**	**126.2(2)**	**131.4(2)**	**127.9(2)**	**125.8(2)**	**130.4(2)**
Distance							
η[j]	3.01(1)	2.88(1)	2.90(1)	2.80(1)	2.74(1)	2.87(1)	2.88(1)
	2.93(1)	**2.92(1)**	**2.91(1)**	**2.81(1)**	**2.79(1)**	**2.93(1)**	**2.89(1)**
δ[k]	−0.17(1)	−0.11(1)	0.21(1)	0.04(1)	−0.26(1)	0.10(1)	0.19(1)
	0.23(1)	**0.08(1)**	**−0.22(1)**	**−0.04(1)**	**0.30(1)**	**−0.14(1)**	**−0.21(1)**

[a] Cremer–Pople puckering amplitude (*21*).
[b] Ideal chair conformation has $\theta = 0$.
[c] Bold numbers are the values of the PIZ inclusion complex.
[d] Torsion angles ϕ and ψ at glycosidic O4, defined as O5(n)—C1(n)—O4($n-1$)—C4($n-1$) and C1(n)—O4($n-1$)—C4($n-1$)—C3($n-1$), respectively.
[e] Torsion angle O5—C5—C6—O6.
[f] Values for sites A and B of the two-fold disordered O61 and O62 with the occupancy factors 0.59, 0.41 and 0.76, 0.24, respectively (PYA).
[g] Values for sites A and B of the two-fold disordered O61 with the occupancy factors 0.57 and 0.43, respectively (PIZ).
[h] Tilt angle, defined as the angle between the O4-plane and the planes through C1(n), C4(n), O4(n) and O4($n-1$).
[i] Angle at each glycosidic O4: O4($n+1$)—O4(n)—O4($n-1$).
[j] Distance O3(n)···O2($n+1$).
[k] Deviation of O4 atoms from the least-squares plane through the seven O4 atoms.

Inclusion geometry and host–guest interactions

In **1**, the disordered PYA molecule (occupancy 0.5) with amide group pointing up is totally included above the O4-plane in the β-CD cavity. The pyrazine centre displaces upwards by 1.15(1) Å from the β-CD O4-centre and inclines by 63.8(5)° against the O4-plane (Figure 2(a)). The PYA molecule is maintained in position by hydrogen bonding with the surrounding β-CD OH groups and water sites within a distance range of 2.71(1)–3.44(1) Å: N1Y···W3; N2Y···W1; N2Y···O22($-x+1$, $y+0.5$, $-z+1$); N3Y···O35(x, $y-1$, z); N3Y···O65($-x$, $y-0.5$, $-z$); N3Y···W5(x, $y-1$, z); O1Y···O25 (x, $y-1$, z); O1Y···O35(x, $y-1$, z); and O1Y···O65($-x$, $y-0.5$, $-z$) (Table 3, Figure 2(a)). In **2**, the PIZ molecule and water site W1 are mutually exclusive, i.e. they do not exist concurrently in the β-CD cavity. The PIZ molecule is mostly located beneath the β-CD O4-plane, except for atom N1Z that is above the O4-plane. The PIZ centre displaces by 0.76(1) Å from the β-CD O4-centre and the PIZ plane (passing through atoms C1—C2—C3—C4) inclines by 39(1)° against the O4-plane (Figure 2(b)). The PIZ molecule is sustained in position by several hydrogen bonds with N···O distances of 2.70(2)–3.50(4) Å: N1Z···W2; N1Z···W3; N2Z···O22($-x$, $y+0.5$, $-z+1$); N2Z···O32($-x$, $y+0.5$, $-z+1$); and N2Z···O62(x, $y+1$, z) (Table 4, Figure 2(b)). The present inclusion complexes in the solid state are mainly stabilised by indirect hydrogen bonds between the guest and the symmetry-related β-CD OH groups and water sites; no direct host–guest interactions exist.

Crystal packing and hydrogen-bonding network

In the crystal lattice, the β-CD–PYA and β-CD–PIZ inclusion complexes exhibit the same packing mode of herringbone (*22*) that is established from the total inclusion of PYA/PIZ in the β-CD cavity. This is frequently observed in the CD crystal structures (*3*). From the survey of Cambridge Structural Database (ConQuest Version 1.9, 2007 Release) (*23*), there are 471 CD crystal structures deposited, which are predominated by 287 native and 86 methylated CDs. Considering only the native and methylated CDs crystallising in the monoclinic space group $P2_1$, about 60 out of 143

Table 3. Possible hydrogen bonding in the β-CD·0.5pyrazinamide·5.5H_2O inclusion complex (**1**) with O···O and N···O separations ≤3.5 Å.

Interaction	Distance (Å)	Interaction	Distance (Å)
β-CD–β-CD		β-CD–H_2O	
O31···O62B[a]	2.89(2)	O21···W4[b]	2.83(1)
O31···O33[b]	3.43(1)	O61A···W2[c]	2.86(1)
O31···O24[b]	3.30(1)	O61B···W3	2.88(3)
O61A···O23[b]	2.92(1)	O22···W1[b]	2.86(5)
O61A···O27[c]	2.89(1)	O32···W1[b]	3.07(4)
O61B···O26[c]	3.11(1)	O32···W2[b]	2.83(1)
O61B···O36[c]	2.60(2)	O52···W2[c]	3.31(1)
O22···O62B[a]	3.00(1)	O62A···W1[c]	2.78(5)
O62A···O35[c]	2.76(1)	O62A···W2[c]	2.69(2)
O62B···O34[c]	3.46(2)	O62B···W1[c]	2.88(5)
O23···O37[b]	2.75(1)	O62B···W2[c]	3.45(2)
O64···O57[d]	3.03(1)	O33···W4[e]	2.82(1)
O64···O67[d]	2.88(1)	O53···W4[c]	3.01(1)
O67···O54[f]	3.42(1)	O63···W4[c]	3.01(1)
O67···O56[g]	3.19(1)	O63···W7[h]	2.82(1)
β-CD–PYA		O24···W4	2.76(1)
O22···N2Y[b]	3.12(2)	O34···W4	3.40(1)
O25···O1Y[i]	2.71(1)	O34···W7[d]	2.91(1)
O35···O1Y[i]	3.29(1)	O64···W5[j]	2.82(1)
O35···N3Y[i]	3.19(1)	O65···W6	2.81(1)
O65···O1Y[k]	3.44(1)	O26···W5	2.75(1)
O65···N3Y[k]	2.98(1)	O26···W3[i]	2.67(2)
PYA–H_2O		O36···W3[i]	3.24(2)
N1Y···W3	3.40(3)	O56···W6	3.08(1)
N2Y···W1	2.90(6)	O66···W3	3.18(2)
N3Y···W5[c]	3.37(1)	O66···W6	2.85(1)
H_2O–H_2O		O66···W5[c]	2.92(1)
W3···W5[c]	3.38(2)	O27···W7	2.72(1)
W6···W7[g]	2.82(1)	O67···W6[g]	2.81(1)

[a] $-x+1, y+0.5, -z+1$.
[b] $-x+1, y-0.5, -z+1$.
[c] $x, y-1, z$.
[d] $x, y, z-1$.
[e] $-x+1, y-0.5, -z$.
[f] $x, y, z+1$.
[g] $-x, y-0.5, -z+1$.
[h] $x, y-1, z-1$.
[i] $x, y+1, z$.
[j] $-x, y-0.5, -z$.
[k] $-x, y+0.5, -z$.

Table 4. Possible hydrogen bonding in the β-CD·0.5piperazine ·7.2H_2O inclusion complex (**2**) with O···O and N···O separations ≤3.5 Å.

Interaction	Distance (Å)	Interaction	Distance (Å)
β-CD–β-CD		O61A···W1[a]	2.91(3)
O31···O33[b]	3.28(1)	O32···W1[b]	2.88(3)
O61A···O23[b]	2.97(1)	O52···W1[a]	3.31(3)
O61A···O27[a]	2.83(2)	O62···W1[a]	2.71(3)
O61B···O26[a]	3.31(2)	O33···W4[c]	2.84(1)
O61B···O36[a]	2.56(2)	O53···W4[a]	2.94(1)
O32···O52[d]	3.44(1)	O63···W4[a]	3.17(1)
O62···O35[a]	3.17(1)	O63···W7[e]	2.64(3)
O23···O61A[d]	2.97(1)	O63···W8[e]	2.88(1)
O23···O37[b]	2.81(1)	O24···W4	2.74(1)
O64···O57[f]	3.10(1)	O34···W4	3.48(1)
O64···O67[f]	2.79(1)	O34···W7[f]	3.07(5)
O67···O56[g]	3.32(1)	O34···W8[f]	2.87(1)
β-CD–PIZ		O64···W5	2.72(1)
N2Z···O22[d]	2.70(2)	O25···W3[h]	2.85(2)
N2Z···O32[d]	2.93(2)	O25···W10[i]	2.90(3)
N2Z···O62[h]	3.07(3)	O35···W3[h]	3.05(3)
PIZ–H_2O		O35···W6[j]	2.89(2)
N1Z···W2	2.83(4)	O65···W6	2.73(1)
N1Z···W3	3.50(4)	O65···W9[k]	2.88(2)
H_2O–H_2O		O65···W10[k]	2.68(3)
W2···W6[l]	2.92(5)	O26···W5[j]	2.84(1)
W3···W6[I]	3.03(3)	O56···W9[k]	3.13(3)
W4···W7[f]	3.35(4)	O66···W2	2.88(4)
W5···W6	2.92(2)	O66···W5[l]	3.21(2)
W5···W11[i]	2.79(4)	O66···W9[k]	3.12(2)
W8···W9[h]	2.83(2)	O66···W11[k]	2.34(3)
W8···W10[h]	2.64(3)	O27···W7	2.83(4)
W8···W11[h]	2.98(3)	O27···W8	2.73(1)
W10···W11	2.66(4)	O27···W11[h]	3.13(4)
β-CD–H_2O		O37···W7	3.38(3)
O21···W4[b]	2.84(1)	O67···W9	2.87(2)
O51···W7[a]	3.31(4)	O67···W10	2.82(3)

[a] $x, y-1, z$.
[b] $-x, y-0.5, -z+1$.
[c] $-x, y-0.5, -z+2$.
[d] $-x, y+0.5, -z+1$.
[e] $x, y-1, z+1$.
[f] $x, y, z+1$.
[g] $-x+1, y-0.5, -z+1$.
[h] $x, y+1, z$.
[i] $x, y+1, z+1$.
[j] $-x+1, y+0.5, -z+2$.
[k] $-x+1, y+0.5, -z+1$.
[l] $-x+1, y-0.5, -z+2$.

structures that have the symmetry-related CD planes in an acute angle with the two-fold screw axis prefer the herringbone packing feature.

The crystal structures of both complexes are stabilised by extensive intermolecular β-CD–β-CD, β-CD—H_2O and H_2O—H_2O hydrogen-bonding networks with similar patterns (Tables 3 and 4). Some β-CD O6—H groups bridge O2—H to O3—H, or O5 to O6—H groups of the adjacent β-CDs: O26(x, $y-1$, z)···O61B···O36(x, $y-1$, z); O57(x, y, $z-1$)···O64···O67(x, y, $z-1$) for both **1** and **2**. Some water sites link O2—H to O3—H, or O5 to O6—H groups: O22···W1···O32, O24···W4···O34, O26···W3···O36 and O52···W2···O62A/B for **1** and O24···W4···O34, O25···W3···O35, O27···W7···O37, O52···W1···O62, O53···W4···O63 and O56···W9···O66 for **2** (Tables 3 and 4). Several water clusters fill the intermolecular spaces between the β-CD macrocycles: W3, W5 and W6, W7 in **1** and W4, W7 and W2, W3, W5, W6, W8–W11 in **2** (Tables 3 and 4). Because the present X-ray diffraction analysis does not give the hydrogen atoms of β-CD OH groups and water molecules, structural details of hydrogen bonds cannot be obtained. By contrast, neutron diffraction permits accurate determination of the H-atom positions, providing the CD hydrates an excellent

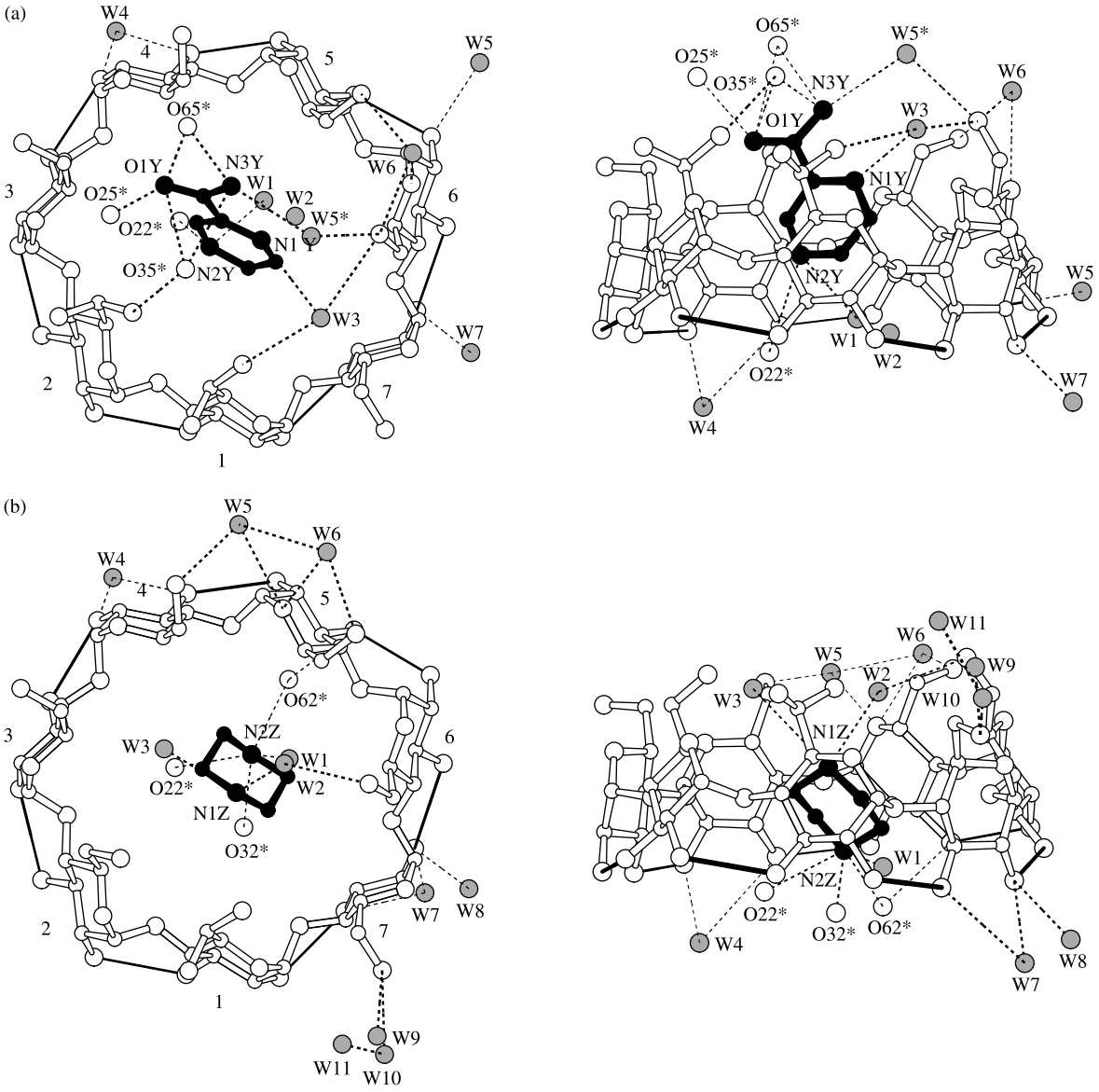

Figure 2. Ball-and-stick representation of (a) β-CD–PYA and (b) β-CD–PIZ inclusion complexes; top views on the left and side views on the right. Circular geometry of β-CD is stabilised by intramolecular, interglucose O3(n)···O2($n+1$) hydrogen bonds (solid lines). For clarity, β-CDs are shown as white ball-and-stick, drugs as black balls, water sites as grey balls and hydrogen atoms are not shown. O—H···O hydrogen bonds are indicated by dashed lines. The symmetry-related oxygen atoms of β-CD and the water molecules hydrogen bonding to drugs are marked with a star (see Tables 3 and 4 for more details). Drawn with MOLSCRIPT (*35*).

model system for detailed study of hydrogen bonding in biological structures (*24*).

β-CD inclusion complexes in the gas phase

Potential energy surface

Figure 3 displays the potential energy surfaces of the β-CD inclusion complexes in the gas phase obtained by PM3 calculations. The PM3 energies (i.e. formation energies) of the free β-CD, PYA and PIZ molecules are -6097.95, -2.14 and $-11.04\,\mathrm{kJ\,mol^{-1}}$, respectively. The β-CD–PYA complexes with amide group both pointing up (β-CD–PYA(u)) and pointing down (β-CD–PYA(d)) are comparatively stable as shown by the binding energies of -22.28 and $-25.29\,\mathrm{kJ\,mol^{-1}}$. The β-CD–PYA(u) complex with PYA placing at 0.5 Å above the β-CD O4-plane is stabilised by N3Y···O66 hydrogen bond, whereas the β-CD–PYA(d) complex with PYA placing at 2.0 Å below the β-CD O4-plane is maintained by O1Y···O23 hydrogen bond (Figure 4). The corresponding N···O and O···O distances are 3.35 and 3.26 Å, respectively. The potential energy surface of the β-CD–

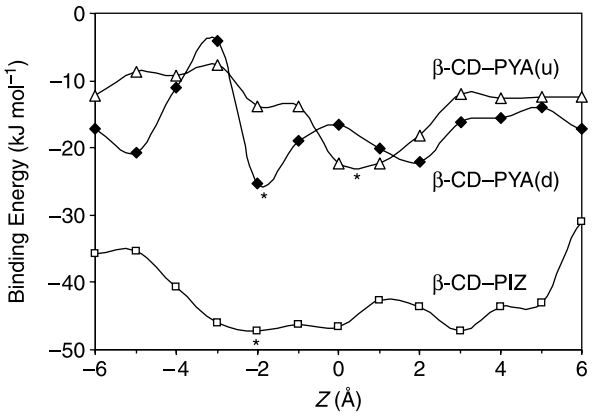

Figure 3. Potential energy surfaces of the β-CD inclusion complexes with PYA (β-CD–PYA(u) and β-CD–PYA(d)) and PIZ (β-CD–PIZ). Letters u and d denote the two possible orientations of PYA amide group pointing up and down. Distance *Z* is measured from the centre-to-centre of host β-CD and guest drug (see also Scheme 2). The global minimum of the potential energy surface is marked with a star.

PIZ complex is shallower and has a greater number of comparable local minima than those of the β-CD–PYA(u) and β-CD–PYA(d) complexes. There are three comparatively stable inclusion geometries ($Z = -2.0$, 0 and 3.0 Å) that the PIZ molecule fits the β-CD cavity almost equally well; the discrepancy in the binding energy is $\leq 0.7\,\text{kJ mol}^{-1}$ (Figure 3). At the global minimum ($Z = -2.0$ Å), the β-CD–PIZ complex sustained by van der Waals forces with binding energy of $-47.28\,\text{kJ mol}^{-1}$ is more energetically favourable than the β-CD–PYA(u) and β-CD–PYA(d) complexes by 25 and 22 kJ mol^{-1}, respectively. In the gas phase that is free from water and crystal-lattice effects, the three inclusion complexes are stabilised by the direct host–guest interactions.

Conformational flexibility

The three PM3-optimised β-CD structures are completely different from one another and from the corresponding crystal structure. They are not superimposable as shown by large rms deviations in the β-CD backbone of 2.27–2.79 Å (O6 atoms are not considered for the calculation; see their structural overlays in Figure 4). The β-CD macrocycles in the gas phase exhibit a distorted 'round' conformation to better accommodate the PYA and PIZ molecules as indicated by O3(n)···O2($n+1$) distances of 2.75–2.77 Å, except for O37···O21 distances of 3.21–3.26 Å. The present finding of β-CD conformational flexibility in the gas phase reflects the importance of induced-fit process (*25*) in the formation of CD inclusion complexes. This is consistent with the results previously obtained by various techniques, e.g. in the gas phase by molecular mechanics calculation (*26*), in the solution by molecular dynamics simulation (*27*) and NMR spectroscopy (*28*), and in the solid phase by crystallography (*29*) (refer to the most recent review (*30*) and references cited therein).

Comparisons between the crystallographic and theoretical results revealing the CD conformational flexibility have been previously reported. The most recent study on the inclusion complexes of α-CD with halogenbenzoic acids using Austin Model 1 (AM1) calculations shows the change in CD ring upon the inclusion of the various sizes of guest molecules (*31*). Other older studies employing different computational methods have been reviewed: α-CD by molecular mechanics and molecular dynamics simulations (*30*), and α- and β-CDs by quantum chemical calculations, for example, AM1, PM3, *ab initio* and density functional theory methods (*32*).

Conclusions

The inclusion complexes of β-cyclodextrin (β-CD) with pyrazinamide (PYA) and piperazine (PIZ) have been investigated both in the solid phase by single-crystal X-ray diffraction analysis and in the gas phase by semi-empirical PM3 calculation.

- In the crystalline state, the β-CD molecular conformation, hydration pattern and crystal packing are similar, but the inclusion geometries of the drug molecules are different. The β-CD macrocycles adopt a 'round' conformation sustained by intramolecular, interglucose O3(n)···O2($n+1$) hydrogen bonds and their O6—H groups are systematically hydrated by water molecules. The disordered PYA molecule with amide group directed up is situated at 1.15(1) Å above the O4-plane in the β-CD cavity, whereas the disordered PIZ molecule is located at 0.76(1) Å below the O4-plane. Both inclusion complexes in the solid state are mainly stabilised by indirect hydrogen bonds between the guest and the symmetry-related β-CD OH groups and water sites; no direct host–guest interactions exist.
- The inclusion scenario has changed in the gas phase that is free from water and crystal-lattice effects. The PM3 calculations reveal that the host β-CD macrocycle in the gas phase is more flexible and hence distorted from the normal circular conformation in the crystalline phase to better accommodate the guest molecule. Two inclusion geometries of the PYA molecule are comparatively stable with the binding energies of -22.28 and $-25.29\,\text{kJ mol}^{-1}$: pyrazine situated at 0.5 Å above the β-CD plane with amide group pointing up and

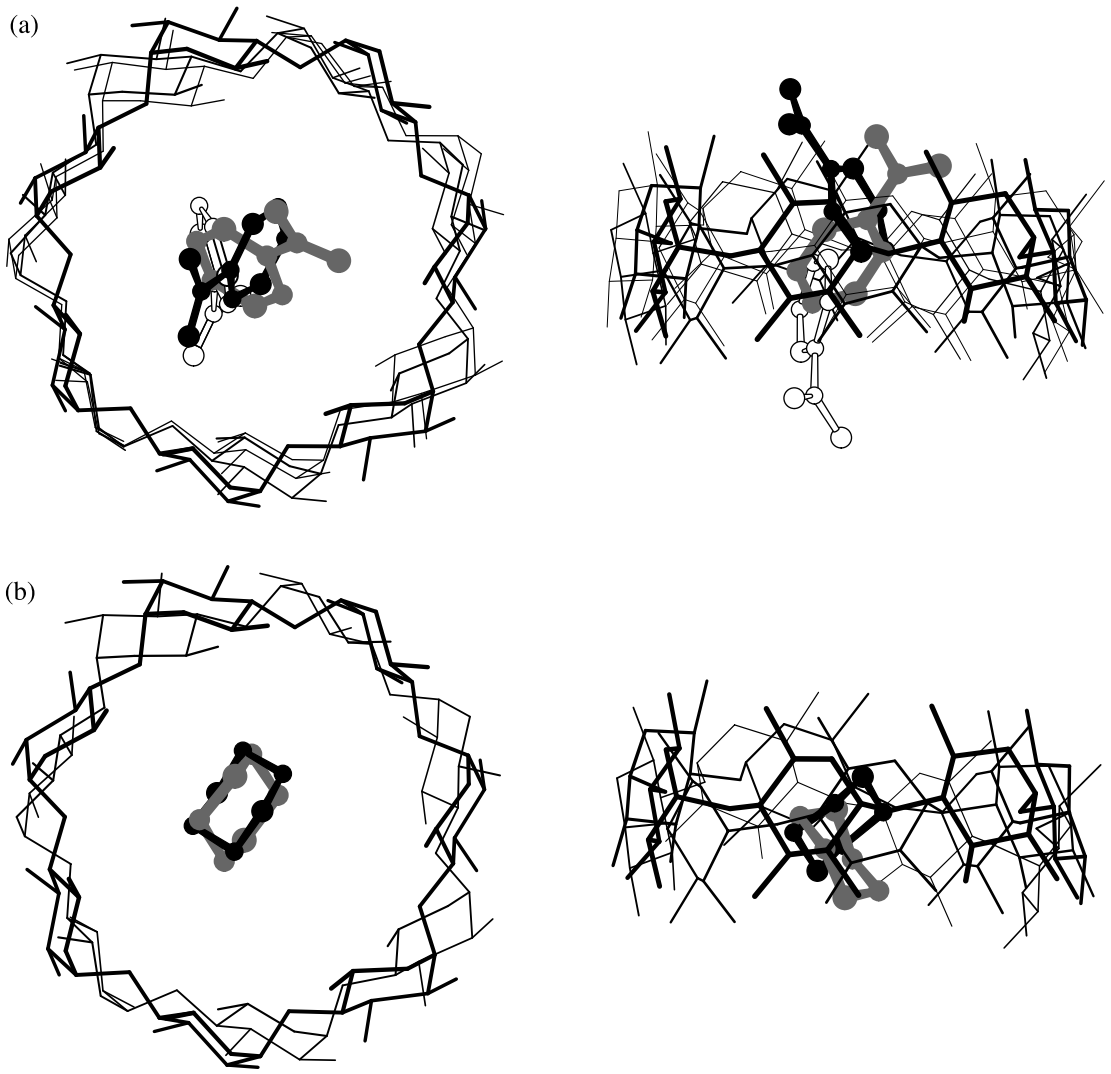

Figure 4. Structural overlays of the β-CD inclusion complexes deduced from X-ray analysis and PM3 calculation; top views on the left and side views on the right. Crystal structures are indicated by the thickest line for β-CDs and by the black ball-and-stick model for drugs. PM3-optimised structures are shown by a moderately thick line for β-CD of the PYA(u) and PIZ complexes, thinnest line for β-CD of the PYA(d) complex and ball-and-stick models in grey for PYA(u) and PIZ and in white for PYA(d) molecules. For clarity, all hydrogen and β-CD O6 atoms are omitted. Drawn with MOLSCRIPT (*35*).

pyrazine located at 2.0 Å below the β-CD plane with amide group pointing down. The PIZ molecule residing at 2.0 Å beneath the β-CD plane gives a more stable complex than does the PYA molecule by 22–25 kJ mol^{-1}. In the gas phase, the PYA and PIZ molecules are sustained in the β-CD cavity by direct host–guest interactions: O···O, N···O hydrogen bonds and van der Waals forces. The CD conformational flexibility facilitating the recognition and induced fit (*24*) between the host CD and guest molecules in the gas phase is more pronounced than in the solid phase, reflecting the dynamics of the inclusion process.

Acknowledgements

We are grateful to the Thailand Research Fund through the Senior Research Scholar Program (Grant number RTA 4880008). This work was partially supported by the Ratchadaphiseksomphot Endowment Fund of Chulalongkorn University through the Materials Chemistry and Catalysis Research Unit to T. Aree. We also thank the Austrian-Thai Centre (ATC) for Computer-Assisted Chemical Education and Research in Bangkok for providing computing facilities.

References

(1) Saenger, W. *Angew. Chem. Int. Ed. Engl.* **1980**, *19*, 344.
(2) Szejtli, J. *Cyclodextrins and Their Inclusion Complexes*; Akademiai Kiado: Budapest, Hungary, 1982.

(3) Harata, K. *Chem. Rev.* **1998**, *98*, 1803.
(4) Duchêne, D., Ed.; *Cyclodextrins and Their Industrial Uses*; Editions de Santé: Paris, France, 1987.
(5) Frömming, K.-H.; Szejtli, J. *Cyclodextrins in Pharmacy*; Kluwer Academic Publishers: Dordrecht, The Netherlands, 1994.
(6) Vinay, R. Oral Cyclodextrin Complexes of Antituberculosis Drugs. PCT Patent WO/2005/074937, 18 August 2005.
(7) Frömming, K.-H.; Wedelich, V.; Mehnert, W. *J. Inclusion Phenom.* **1984**, *2*, 605.
(8) Frömming, K.-H.; Wedelich, V.; Mehnert, W.; Lange, A.; Hosemann, R. *Arch. Pharm.* **1987**, *320*, 294.
(9) Sheldrick, G.M. *SHELXTL, Version 5.0*; Siemens Analytical X-ray Instruments Inc., Madison, WI: USA, 1996.
(10) Sheldrick, G.M. *SADABS, Programme for Empirical Absorption Correction of Area Detector Data*; University of Göttingen: Göttingen, Germany, 1996.
(11) Egert, E.; Sheldrick, G.M. *Acta Crystallogr.* **1985**, *A41*, 262.
(12) Aree, T.; Schulz, B.; Reck, G. *J. Inclusion Phenom. Macrocycl. Chem.* **2003**, *47*, 39.
(13) McRee, D.E. *J. Struct. Biol.* **1999**, *125*, 156.
(14) Sheldrick, G.M.; Schneider, T.R. *Methods Enzymol.* **1997**, *277*, 319.
(15) Nardelli, M. *J. Appl. Crystallogr.* **1995**, *28*, 659.
(16) Spek, A.L. *PLATON, A Multipurpose Crystallographic Tool*; Utrecht University: Utrecht, The Netherlands, 1998.
(17) CCDC no. 670911 (β-CD--PYA complex) and 670912 (β-CD--PIZ complex) contain the supplementary crystallographic data for this paper. These data can be obtained free of charge from The Cambridge Crystallographic Data Centre via www.ccdc.cam.ac.uk/data_request/cif.
(18) Walters, P.; Stahl, M. *BABEL, Version 1.3, Programme for the Interconversion of File Formats Used in Molecular Modelling*; University of Arizona: USA, 1992–1996.
(19) Frisch, M.J.; Trucks, G.W.; Schlegel, H.B.; Scuseria, G.E.; Robb, M.A.; Cheeseman, J.R.; Montgomery, J.A.; Vreven, T.; Kudin, K.N.; Burant, J.C.; et al. *GAUSSIAN03, Revision B.02*; Gaussian, Inc. Pittsburgh, PA, 2003.
(20) Jeffrey, G.A. *An Introduction to Hydrogen Bonding*; Oxford University Press: Oxford, UK, 1997.
(21) Cremer, D.; Pople, J.A. *J. Am. Chem. Soc.* **1975**, *97*, 1354.
(22) Saenger, W. *Isr. J. Chem.* **1985**, *25*, 43.
(23) Allen, F.H. *Acta Crystallogr.* **2002**, *B58*, 380.
(24) Jeffrey, G.A.; Saenger, W. *Hydrogen Bonding in Biological Structures*; Springer-Verlag: Berlin, Germany, 1991.
(25) Koshland, D.E., Jr. *Sci. Am.* **1973**, *229*, 52.
(26) Lipkowitz, K.B. *J. Org. Chem.* **1991**, *56*, 6357.
(27) Raffaini, G.; Ganazzoli, F. *Chem. Phys.* **2007**, *333*, 128.
(28) Ishizu, T.; Hirata, C.; Yamamoto, H.; Harano, K. *Magn. Reson. Chem.* **2006**, *44*, 776.
(29) Aree, T.; Hoier, H.; Schulz, B.; Reck, G.; Saenger, W. *Carbohydr. Res.* **2000**, *328*, 399.
(30) Dodziuk, H. *J. Mol. Struct.* **2002**, *614*, 33.
(31) Pumera, M.; Rulíšek, L. *J. Mol. Model.* **2006**, *12*, 799.
(32) Liu, L.; Guo, Q.-X. *J. Inclusion Phenom. Macrocycl. Chem.* **2004**, *50*, 95.
(33) Laugier, J.; Bochu, B. *GRETEP, Version 2: Grenoble Thermal Ellipsoid Plot Programme. Laboratoire des Matériaux et du Génie Physique*; Ecole Nationale Supérieure de Physique de Grenoble: St Martin d'Hères, France, 2003.
(34) Cason, C.J. POV-RAY for Windows. Version 3.6., 2003.
(35) Kraulis, P.J. *J. Appl. Crystallogr.* **1991**, *24*, 946.